Published in final edited form as:
Pediatr Radiol. 2011 June ; 41(6): . doi:10.1007/s00247-010-1932-z.

Improved Cardiovascular Flow Quanfitication with Time-Resolved Volumetric Phase-Contrast MRI

Albert Hsiao, MD, PhD
Resident Physician Department of Radiology 300 Pasteur Drive, Room H3630 Stanford, CA 94305 ph: (858) 335-2173 fax: (650) 723-1909

Marcus T. Alley, PhD
Department of Radiology 300 Pasteur Drive Stanford, CA 94305

Payam Massaband, MD
Department of Radiology 300 Pasteur Drive Stanford, CA 94305

Robert J. Herfkens, MD
Lucas MR Building, P261 1201 Welch Road Stanford, CA 94305

Frandics P. Chan, MD, PhD
Department of Radiology Grant S066 300 Pasteur Drive Stanford, CA 94305

Shreyas S. Vasanawala, MD, PhD
Department of Radiology 725 Welch Rd. Rm 1679 MC 5913 Stanford, CA 94305-5654 ph: (650) 724-9824 fax: (650) 723-8402

Abstract

Background: Cardiovascular flow is commonly assessed with two-dimensional, phase contrast (2D PC-MRI). However, scan prescription and acquisition over multiple planes is lengthy, often requires direct physician oversight, and has inconsistent results. Time-resolved volumetric PC-MRI (4D flow) may address these limitations.

Objective: We assess the degree of agreement and internal consistency between 2D and 4D flow quantification in our clinical population.

Method: Software enabling flow calculation from 4D flow was developed in Java. With IRB approval and HIPAA compliance, eighteen consecutive patients without shunts were identified who underwent both (a) conventional 2D PC-MRI of the aorta and main pulmonary artery and (b) 4D flow imaging. Aortic and pulmonary flow rates were assessed with both techniques.

Results: Both methods showed general agreement in flow rates (ρ: 0.87-0.90). Systemic and pulmonary arterial flow rates were well-correlated (ρ: 4D 0.98-0.99, 2D 0.93), but more closely matched with 4D ($p<0.05$, *Brown-Forsythe*). Pulmonary flow rates were lower than systemic rates for 2D ($p<0.05$, *two-sample t-test*). In a sub-analysis of patients without pulmonary or aortic regurgitation, 2D showed improved correlation of flow rates while 4D phase-contrast remained tightly correlated (ρ: 4D 0.99-1.00, 2D 0.99).

Conclusion: 4D PC-MRI demonstrates greater consistency than conventional 2D PC-MRI for flow quantification.

(Corresponding author) alhsiao@stanford.eduvasanawala@stanford.edu.

Keywords

blood flow; magnetic resonance imaging; imaging

Introduction

Two-dimensional, phase-contrast magnetic resonance imaging (2D PC-MRI) is a commonly employed and proven clinical tool for the evaluation of cardiovascular blood flow [1-3]. Specifically, in congenital heart disease, the cardiac output, regurgitant fraction, and shunt ratio evaluated to guide subsequent intervention. Given its clinical utility, recent efforts have aimed to shorten the acquisition time of 2D PC-MRI while preserving accuracy [4, 5]. Nevertheless, scan prescription and acquisition of multiple planes for comprehensive evaluation of flow is a lengthy process, which requires a skilled operator with knowledge of cardiovascular anatomy in the context of congenital heart defects. Furthermore, in clinical practice, the results of 2D PC-MRI are often inconsistent, even with correction techniques to address eddy-current-related phase-offsets [6]. Volumetric, time-resolved phase-contrast imaging (4D flow) [3, 7, 8] has potential for overcoming some of these limitations because of the volumetric nature of its acquisition.

While the 2D technique primarily acquires images of the perpendicular component of velocity, the 4D method acquires velocity components in all three spatial dimensions. Like conventional 2D PC-MRI, a magnitude image series can be reconstructed to visualize anatomic structures and delineate the cross-sectional area of the flow lumen. Arbitrary slice planes can be retrospectively reconstructed and processed computationally to evaluate flow in any large vessel of interest. Since an entire volume is prescribed, rather than a plane defined by a particular anatomic structure, this simplifies the acquisition process and thereby reduces the operator-dependence characteristic of 2D PC-MRI.

Using 4D PC-MRI, several groups have described a range of pathological flow patterns associated with various cardiovascular diseases, which are otherwise not apparent on conventional imaging [9-12]. However, the clinical utility of this method has until now been limited by prohibitively long acquisition times. Recent improvements in adapting parallel imaging have reduced scan time and have lowered the barrier to utilization [13]. However, given its high-dimensional nature, this vector field data is difficult to visually assess with currently available image review systems. Furthermore, there is currently no clinical system for quantification of flow across vessels of interest. Thus, a significant barrier to clinical use of this technique is the lack of efficient computational tools.

While quantitative flow assessment by 2D PC-MRI has previously been extensively validated in phantom models and clinical populations, more work needs to be done to validate measurements obtained from 4D flow. A few groups have shown promising preliminary results in healthy volunteers. Earlier works have confirmed strong correlations between 4D flow and 2D PC-MRI velocity and volumetric flow measurements [14, 15]. Another work showed consistency in 4D flow measurements obtained at each of the cardiac valves[16]. Recently, the quantitative accuracy of volumetric approach has been evaluated in tetralogy patients after repair, showing good agreement with 2D assessment [17]. We therefore sought to develop algorithms with a platform-independent implementation to permit flow quantification from 4D flow datasets, determine the degree of agreement between 2D and 4D methods, and establish the relative consistency of aortic and pulmonary flow measurements by both methods in a clinical setting.

Methods

Patient population

With institutional review board approval and HIPAA compliance, we retrospectively identified patients referred for MRI at our children's hospital who underwent both conventional 2D phase-contrast sequences of the aorta and pulmonary arteries as well as a 4D flow sequence from March-December, 2009. For the purposes of devising an internal control, patients with known shunts demonstrated either by echocardiography or prior MRI examinations on were excluded. After reviewing patient charts, eighteen consecutive patients were identified. Measurements of the flow rates in the proximal aorta and main pulmonary artery were obtained with each technique, further described below. Table 1 summarizes the patient demographics and acquisition parameters.

Image acquisition

All imaging was performed on a 1.5-T TwinSpeed MRI Scanner (GE Healthcare, Milwaukee, WI) with 150 T/ms maximum slew rate, 40 mT/min gradients, and vector ECG gating. In ten patients, the 2D phase-contrast acquisition was performed following contrast-enhanced angiography with intravenous contrast (single or double-dose, gadobenate dimeglumine or gadopentetate dimeglumine) routinely performed as part of our cardiac MRI protocol. In the remaining eight patients, the 2D acquisition preceded administration of contrast. 4D flow was always performed as the last sequence of each patient's exam.

2D PC-MRI scan planes were prescribed by board-certified radiologists with dedicated training in pediatric cardiovascular imaging. 2D phase-contrast images were acquired with a GRE sequence (FastCard), with echo times (TE) averaging 2.8 ms, repetition times (TR) averaging 5.3 ms, 6-10 views per segment depending on patient heart rate, flip angle of 20°, and slice thickness of 8-10 mm. Retrospective ECG gating was used and signal reception was done using an eight-channel phased-array cardiac coil (GE Healthcare). Parallel-imaging was not employed. The velocity encoding (v_{enc}) parameter was chosen at the time of each study by starting at 150 cm/s and increasing iteratively to avoid aliasing. In the six patients capable of breath-holding, a single signal average (1 NEX) breath-hold acquisition was performed. Otherwise, a 3 or 4 signal-average free-breathing acquisition was used to reduce respiratory artifact. After performing appropriate localizers, acquisition times were approximately 20 seconds for breath-held and 1 minute for free-breathing examinations for each plane of imaging. At least two planes at each valve were acquired with additional acquisitions at the jets when regurgitation or stenoses were present.

The 4D flow acquisition was performed using a SPGR-based sequence with flow-encoding along all three directions and a parallel imaging outer reduction factor of 2 in the phase encode direction [15, 18]. Respiratory compensation with k-space phase reordering (EXORCIST, GE Healthcare) was employed without respiratory gating or navigation. Velocity-encoding parameters were selected to avoid aliasing and generally matched or exceeded the parameter used in the 2D acquisitions. A flip angle of 15°, average TE of 1.7 ms, average TR of 4.5 ms and 2-4 tetrahedral encodes per segment were used. Images were reconstructed with generalized autocalibrating partially parallel acquisitions (GRAPPA) and zero-filling in the through-plane direction by a factor of 2. In most cases, we selected a right/left frequency direction, except for two subjects, where we selected a craniocaudal frequency direction. Acquisition times ranged from 9 to 22 minutes with a mean of 15 minutes. Image data were automatically corrected for Maxwell phase effects [19], encoding errors related to gradient field distortions [20], and eddy-current related phase offsets[21].

Image processing

To permit flow quantification, a graphical user interface was developed in Java with the Standard Widget Toolkit (SWT). In this interface, the user navigates through the volume to select a location within a vessel of interest. The software automatically constructs a plane perpendicular to the velocity vector at that location. Reformatted velocity images in this plane are created using nearest-neighbor interpolation, transformed into cylindrical coordinates. The volumetric flow is then computed as the sum of the through-plane velocities in the segmented lumen. Rotational and radial component images are produced solely for visualization of flow in the cross-section, as they do not contribute to net flow. Magnitude images are reformatted with trilinear interpolation.

An example of source and reformatted images from a patient with repaired tetralogy of Fallot is displayed in Figure 1. Within this plane, the user manually defines a segmentation of the vessel lumen, facilitated by views of the radial and rotational velocity components. Flow calculations are computed as the sum of through-plane velocities within the segmented area, averaged over all cardiac phases. The software also provides image processing functions to facilitate visualization by a third-party software called Ensight (CEI, Apex, NC). For the same patient with repaired tetralogy of Fallot, flow curves computed with the software and streamline renderings using Ensight are shown in Figure 2.

Volumetric flow analysis

Quantitative flow measurements were obtained from both 2D and 4D acquisitions matching the level of the aortic and pulmonary valves. In patients without clearly defined valves, such as patients with repaired tetralogy of Fallot, the valve level was approximated in the mid-pulmonary trunk. For 2D phase-contrast data, soft tissue background-corrections were applied to correct for eddy-current-related phase offsets. Segmentations of the vessel lumen and soft tissue background were performed with the commercially-available CV Flow version 4 package on a GE Advantage workstation version 4.2 (GE Healthcare). Each cardiac phase was manually segmented by a board-certified radiologist with subspecialty training in cardiovascular imaging.

4D phase-contrast data was processed by the primary author, a radiology resident at the time of the study. Cross-sectional planes were also selected at the valves. Slice planes were chosen centered on the vessel lumen, oriented perpendicular to flow in early systole. Three alternate methods were used for segmentation. In the first method, a single segmentation was performed at peak systolic flow and propagated to the remaining cardiac phases (subsequently referred to as 4D single phase). In the second method, six additional slice planes were separately selected near the level of the valves by incrementally selecting planes along the length of the vessel, with each new plane separated by approximately one interpolated slice thickness. Each of these were segmented at the phase of peak systolic flow, and propagated to the remaining cardiac phases (4D repeated). The mean of the seven repeated measurements was then used as an estimate of flow rate. In the third method, one slice plane was selected near the level of the valves. Manual-segmentations were performed for each of the cardiac phases (4D multiple phase).

For all 2D and 4D methodologies, plane selection and segmentations were performed while blinded to flow calculations. For 2D phase-contrast, aortic segmentations and flow calculations were performed and recorded for each patient. After one week, the pulmonary vessel segmentations and flow calculations were separately performed and recorded. For 4D phase-contrast, all segmentations were performed for each patient. Tables of flow results were automatically computed without additional user-intervention.

Statistical analysis

Calculations were performed in Excel 2003 (Microsoft, Redmond, WA). The limits of agreement are reported as differences from the mean of 1.96 standard deviations. To evaluate the deviations between systemic (Q_s) and pulmonary (Q_p) flow measurements, the absolute precision was defined as Q_p-Q_s, and assumed to be approximately normal with a mean of zero. The Brown-Forsythe test was used to test the null hypothesis that each pair of imaging and segmentation techniques had the same measurement error.For a sub-population analysis in patients without valvular regurgitation, significant regurgitation was defined as a regurgitant fraction of greater than 20% at either the aortic or pulmonary valve measured by 4D PC-MRI.

In order to detect other possible relationships with Q_p-Q_s, additional tests were performed. Linear regression was used to find associations with continuous factors (age, weight, heart rate, velocity-encoding, matrix-size) and the F-test was used to test for statistically significant relationships. Two-sample, unequal variance t-tests were used to test for relationships with categorical factors (acquisition plane, timing of contrast-administration, use of breath holding in 2D phase-contrast).

Results

Table 2 summarizes the extent of agreement between 2D PC-MRI and each of the segmentation approaches used with 4D PC-MRI. Comparing each of the 4D segmentation techniques to each other, Pearson correlation coefficients ranged between 0.99-1.00. There is close agreement between each of the 4D PC-MRI segmentation techniques, with no statistically significant mean difference in the measured flow rates. The observed mean differences comprised 1-2% of the flow rate. Upper limits of agreement ranged between 0.3-0.4 L/minute, corresponding to less than 10% of the flow rate. Thus, flow measurements from 4D phase-contrast MRI were closely-matched across segmentation techniques.

Comparing 2D to 4D phase contrast measurements, Pearson correlation coefficients ranged between 0.87-0.90. A Bland-Altman plot of this comparison is shown in Figure 3. Flow measurements with 4D flow were slightly lower than measurements obtained with the 2D technique, a difference of 0.3-0.4 L/min, corresponding to an average difference of 6-8%. The magnitude of this difference is similar to that of a previous study of healthy volunteers, where estimated stroke volumes were on average 3% greater with 4D PC-MRI than with 2D PC-MRI [14]. A flow-dependent bias was not observed. The limits of agreement between 2D and 4D methods was comparable to the agreement in a prior study comparing SENSE-accelerated 2D PC-MRI and conventional 2D PC-MRI, which showed upper limits of agreement of 1-2 L/min [4].

Table 3 summarizes the correlation between pulmonary and systemic flow rates measured by each of the 2D and 4D PC-MRI techniques. Bland-Altman plots are shown in figure 4. By 2D phase-contrast, the measured pulmonary flow rates were on average 0.5 L/min or 15% less than the systemic flow rates, a difference that was statistically-significant ($p<0.05$). Put slightly differently, the estimated Q_p/Q_s ratios were widely variable and typically underestimated with a mean of 0.87. They were seen to range between 0.57-1.17 (95% CI) in the absence of a shunt. There was no significant difference in the consistency of Q_p and Q_s measurements between breath-held and free-breathing exams. It is also notable that the limits of agreement between Q_p and Q_s by 2D PC-MRI are comparable to the limits relating 2D PC-MRI and to 4D PC-MRI.

By 4D phase-contrast, pulmonary and systemic flow rates were more closely matched. Pulmonary flow rates were on average 0.1 L/min or 2-4% less than systemic flow rates. The

limits of agreement were similar between each of the 4D segmentation techniques, with the narrowest being either (a) repeated single-phase segmentations (−18% to +12%), or (b) one set of multiple-phase segmentations (−19% to +11%). The measured Q_p/Q_s was accurate with means between 0.96-0.99, depending on segmentation technique, and was weakest when only one single phase segmentation was used. This was a considerable improvement over the range of Q_p/Q_s observed by 2D PC-MRI. The results of linear regression of Q_p and Q_s were also markedly improved over 2D PC-MRI.

To further confirm the improved precision of the 4D phase contrast method, we also employed an analysis of the variance between the Q_p and Q_s measurements (Table 4). There was a statistically significant improvement in absolute precision (Q_p-Q_s) by 4D PC-MRI over 2D PC-MRI when either (a) temporally-resolved, multiple-phase segmentations or (b) repeated single-phase segmentations were used ($p<0.05$). Multiple-phase segmentations also had improved precision over single-phase segmentation measurements ($p<0.05$). These results indicate that the additional labor-intensive effort of segmenting each cardiac phase did manifest in a detectable improvement in precision.

Since non-laminar and accelerating flow patterns are known to decrease the accuracy of phase-contrast flow quantification [22], we further stratified our patient population using the presence of significant valvular regurgitation as a surrogate for complex flow (Table 3). Six of the ten patients that satisfied these criteria also had documented regurgitation of at least moderate severity by Doppler echocardiogram. In the subpopulation without regurgitation, the correlation of 2D PC-MRI measurements of Q_p and Q_s improved. The mean difference was closer to zero with Q_p measuring, 8% less than Q_s, and narrower limits of agreement. The 4D flow measurements remained tightly correlated.

Discussion

In our study, we find that time-resolved, volumetric, phase-contrast MRI is feasible for volumetric flow quantification and demonstrates comparable accuracy and improved precision to 2D phase-contrast MRI. We demonstrate this in a population of patients typically evaluated at our institution, most of whom are referred with complex congenital heart disease. One of the major hurdles for broader utilization of 4D flow in clinical practice has been the lack of available tools for evaluating the resulting data sets. Previous groups have primarily focused on developing tools for visualization of this data [23, 24], but a tailored tool for quantification of flow is also not widely available. The work we present here may serve as a template for future software designed to utilize the quantitative power of this pulse sequence.

A major benefit of the 4D flow approach is the ability to retrospectively interrogate vessels within the prescribed volume. Since the prescription of such a volume does not require detailed anatomic knowledge, it can be readily performed by a technologist without a physician present. Furthermore, it may not be possible to know, prospectively, all of the imaging planes where flow quantification may be useful. We have encountered this issue, for example, in patients with partial anomalous pulmonary venous return. This an issue avoided with the 4D flow approach.

We show the typical range of Q_p/Q_s obtained by 2D phase-contrast when segmentations and background corrections are manually performed, without the influence of subsequent flow calculations. This is shown across the broad range of cardiac outputs encountered in our practice. The limit of agreement between measurements of Q_p and Q_s was found to be relatively wide and is typical of our experience and others in recent years [6, 25]. In the absence of an identifiable shunt, discordant Q_p/Q_s can be confusing and difficult to justify.

Improved precision of measurements by 4D flow is therefore likely to be of significance to both interpreting cardiac imagers and referring clinicians.

Complex flow patterns are frequently observed in patients referred for cardiac MRI. Using valvular regurgitation as a surrogate for complex flow, we performed a sub-analysis of patients without valvular regurgitation and showed 2D PC-MRI measurements of Q_p and Q_s were more closely matched, suggesting that these flow patterns may have an effect. Accelerating, non-laminar flow is a known confounder of phase-contrast flow assessment, and methods that employ even shorter echo times (TE) have been shown to further improve precision, possibly related to decreased intravoxel dephasing and improved temporal resolution [22]. A shortened echo time is not unique to our implementation, but a common feature of 4D PC-MRI. Since slice-direction resolution in 3D imaging is not dependent on the spatial excitation pulse, shorter echo times are possible and the typical tradeoff between temporal resolution and slice thickness is reduced. It is for this reason that finer slice thicknesses are possible the 4D method, which may also better resolve complex flow. In order to obtain equivalent slice thicknesses by 2D phase contrast, temporal resolution may need to be sacrificed.

It is not entirely clear why, in our patient population, we observed improved consistency of flow measurements by 4D PC-MRI. To some extent, this may be influenced by the population we see in our practice, which contains a high proportion of patients with complex flow. Further studies may be helpful to assess whether this level of precision is also observed in other referral populations, and over time, in a greater number of patients. There are a few possible confounding factors, one of which is the use of breath-holding in 2D phase-contrast. Breath-holding was employed for 2D phase-contrast, when possible, to provide a comparison against the current clinical standard. This could affect measurement if a shunt was present, but none of our patients had detectable shunts. Respiratory compensation was used for 4D phase-contrast, but not for 2D. Since there was no significant difference in the consistency of aortic and pulmonary flows in breath-held and free-breathing 2D exams, this is unlikely to be a contributing factor. It is also important to note that in the clinical setting, there is always inherent variability in how the MRI exams are performed, as exams must be tailored for each patient to account for the clinical needs, patient size and heart rate, and available acquisition time. The acquisition parameters therefore are not uniform across all patients, but represent a spectrum typical of modern practice. Since 2D and 4D PC-MRI acquisition parameters were well-matched for each patient, comparison of the two techniques is feasible. Furthermore, the broad range of patients and parameters demonstrate that the findings are robust across a variety of clinical scenarios.

The results presented here raise the possibility that 4D phase-contrast may ultimately be used in place of 2D phase-contrast to expedite workflow and allow the cardiac imager to exercise expertise at the workstation instead of at the scanner. An important factor for whether this will manifest in time-savings relies on the ability to efficiently process the 4D phase-contrast data with software specifically designed to help the cardiac imager to interrogate vessels of interest. Future work may address further development of such software. In addition, it is not presently possible to automatically adjust the velocity-encoding parameter to maximally leverage the velocity-to-noise ratio, and our ongoing work will seek to address this. The current acquisition times are relatively long, but may be further reduced with two-dimensional acceleration instead of one-dimensional acceleration that we have applied in this study. Further work in each of these areas will help to bring this pulse sequence closer to clinical use.

Conclusions

4D PC-MRI is feasible, allows retrospective evaluation of blood flow, and in clinical practice demonstrates greater consistency than conventional 2D PC-MRI for flow quantification.

Bibliography

1. Szolar DH, Sakuma H, Higgins CB. Cardiovascular applications of magnetic resonance flow and velocity measurements. J Magn Reson Imaging. 1996; 6:78–89. [PubMed: 8851410]
2. Higgins CB, Sakuma H. Heart disease: functional evaluation with MR imaging. Radiology. 1996; 199:307–315. [PubMed: 8668769]
3. Pelc NJ, Herfkens RJ, Shimakawa A, et al. Phase contrast cine magnetic resonance imaging. Magn Reson Q. 1991; 7:229–254. [PubMed: 1790111]
4. Lew CD, Alley MT, Bammer R, et al. Peak velocity and flow quantification validation for sensitivity-encoded phase-contrast MR imaging. Acad Radiol. 2007; 14:258–269. [PubMed: 17307658]
5. Korperich H, Gieseke J, Barth P, et al. Flow volume and shunt quantification in pediatric congenital heart disease by real-time magnetic resonance velocity mapping: a validation study. Circulation. 2004; 109:1987–1993. [PubMed: 15066942]
6. Gatehouse PD, Rolf MP, Graves MJ, et al. Flow measurement by cardiovascular magnetic resonance: a multi-centre multi-vendor study of background phase offset errors that can compromise the accuracy of derived regurgitant or shunt flow measurements. J Cardiovasc Magn Reson. 12:5. [PubMed: 20074359]
7. Pelc NJ, Bernstein MA, Shimakawa A, et al. Encoding strategies for three-direction phase-contrast MR imaging of flow. J Magn Reson Imaging. 1991; 1:405–413. [PubMed: 1790362]
8. Alley MT, Napel S, Amano Y, et al. Fast 3D cardiac cine MR imaging. J Magn Reson Imaging. 1999; 9:751–755. [PubMed: 10331775]
9. Markl M, Draney MT, Hope MDMD, et al. Time-Resolved 3-Dimensional Velocity Mapping in the Thoracic Aorta: Visualization of 3-Directional Blood Flow Patterns in Healthy Volunteers and Patients. Journal of Computer Assisted Tomography July/August. 2004; 28:459–468.
10. Hope TA, Markl M, Wigström L, et al. Comparison of flow patterns in ascending aortic aneurysms and volunteers using four-dimensional magnetic resonance velocity mapping. Journal of Magnetic Resonance Imaging. 2007; 26:1471–1479. [PubMed: 17968892]
11. Isoda H, Ohkura Y, Kosugi T, et al. In vivo hemodynamic analysis of intracranial aneurysms obtained by magnetic resonance fluid dynamics (MRFD) based on time-resolved three-dimensional phase-contrast MRI. Neuroradiology. 2009
12. Hope MD, Hope TA, Meadows AK, et al. Bicuspid aortic valve: four-dimensional MR evaluation of ascending aortic systolic flow patterns. Radiology. 255:53–61. [PubMed: 20308444]
13. Peng HH, Bauer S, Huang TY, et al. Optimized parallel imaging for dynamic PC-MRI with multidirectional velocity encoding. Magn Reson Med. 2010; 64:472–480. [PubMed: 20665791]
14. Brix L, Ringgaard S, Rasmusson A, et al. Three dimensional three component whole heart cardiovascular magnetic resonance velocity mapping: comparison of flow measurements from 3D and 2D acquisitions. J Cardiovasc Magn Reson. 2009; 11:3. [PubMed: 19232119]
15. Markl M, Chan FP, Alley MT, et al. Time-resolved three-dimensional phase-contrast MRI. J Magn Reson Imaging. 2003; 17:499–506. [PubMed: 12655592]
16. Roes SD, Hammer S, van der Geest RJ, et al. Flow Assessment Through Four Heart Valves Simultaneously Using 3-Dimensional 3-Directional Velocity-Encoded Magnetic Resonance Imaging With Retrospective Valve Tracking in Healthy Volunteers and Patients With Valvular Regurgitation. Invest Radiol. 2009
17. van der Hulst AE, Westenberg JJ, Kroft LJ, et al. Tetralogy of fallot: 3D velocity-encoded MR imaging for evaluation of right ventricular valve flow and diastolic function in patients after correction. Radiology. 2010; 256:724–734. [PubMed: 20634432]

18. Bammer R, Hope TA, Aksoy M, et al. Time-resolved 3D quantitative flow MRI of the major intracranial vessels: initial experience and comparative evaluation at 1.5T and 3.0T in combination with parallel imaging. Magn Reson Med. 2007; 57:127–140. [PubMed: 17195166]

19. Bernstein MA, Zhou XJ, Polzin JA, et al. Concomitant gradient terms in phase contrast MR: analysis and correction. Magn Reson Med. 1998; 39:300–308. [PubMed: 9469714]

20. Markl M, Bammer R, Alley MT, et al. Generalized reconstruction of phase contrast MRI: analysis and correction of the effect of gradient field distortions. Magn Reson Med. 2003; 50:791–801. [PubMed: 14523966]

21. Walker PG, Cranney GB, Scheidegger MB, et al. Semiautomated method for noise reduction and background phase error correction in MR phase velocity data. Journal of Magnetic Resonance Imaging. 1993; 3:521–530. [PubMed: 8324312]

22. O'Brien KR, Myerson SG, Cowan BR, et al. Phase contrast ultrashort TE: A more reliable technique for measurement of high-velocity turbulent stenotic jets. Magn Reson Med. 2009; 62:626–636. [PubMed: 19488986]

23. Unterhinninghofen R, Ley S, Ley-Zaporozhan J, et al. Concepts for Visualization of Multidirectional Phase-contrast MRI of the Heart and Large Thoracic Vessels. Academic Radiology. 2008; 15:361–369. [PubMed: 18280934]

24. Sørensen TS, Beerbaum P, Körperich H, et al. Three-dimensional, isotropic MRI: a unified approach to quantification and visualization in congenital heart disease. The International Journal of Cardiovascular Imaging (formerly Cardiac Imaging). 2005; 21:283–292.

25. Kilner PJ, Gatehouse PD, Firmin DN. Flow measurement by magnetic resonance: a unique asset worth optimising. J Cardiovasc Magn Reson. 2007; 9:723–728. [PubMed: 17613655]

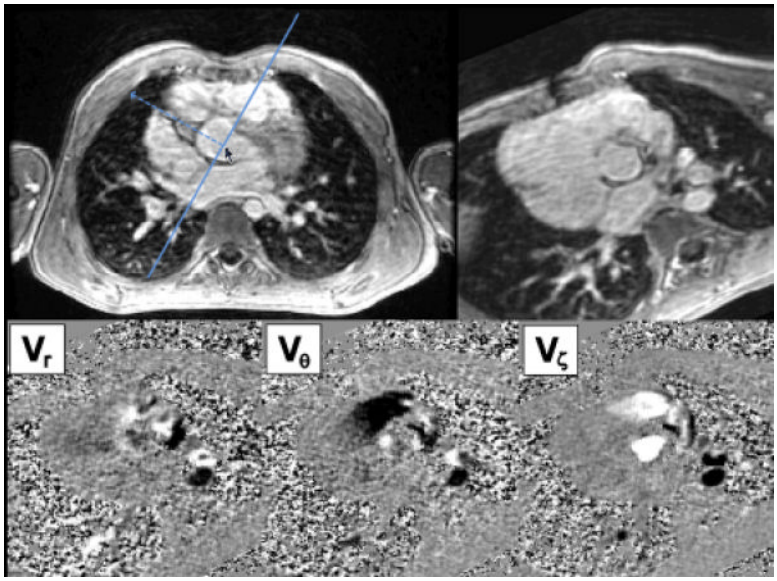

Figure 1.

Cross-sectional images from the 4D flow acquisition, constructed at the plane of the aortic valve at peak-systole. The raw axial image is shown (a) with the location selected by the user to create a cross-section, labeled with an arrow. The software automatically creates a cross-section perpendicular to the direction of flow. The intersection of this plane with the axial image is marked by a blue solid line and the projection of the normal vector is displayed as a dashed line. The reformatted magnitude image (b), radial velocity (v_r), rotational velocity (v_θ) and through-plane velocity (v_ζ) are shown at peak-systole. The net flow is computed as the sum of the through-plane velocities in the segmented vessel lumen.

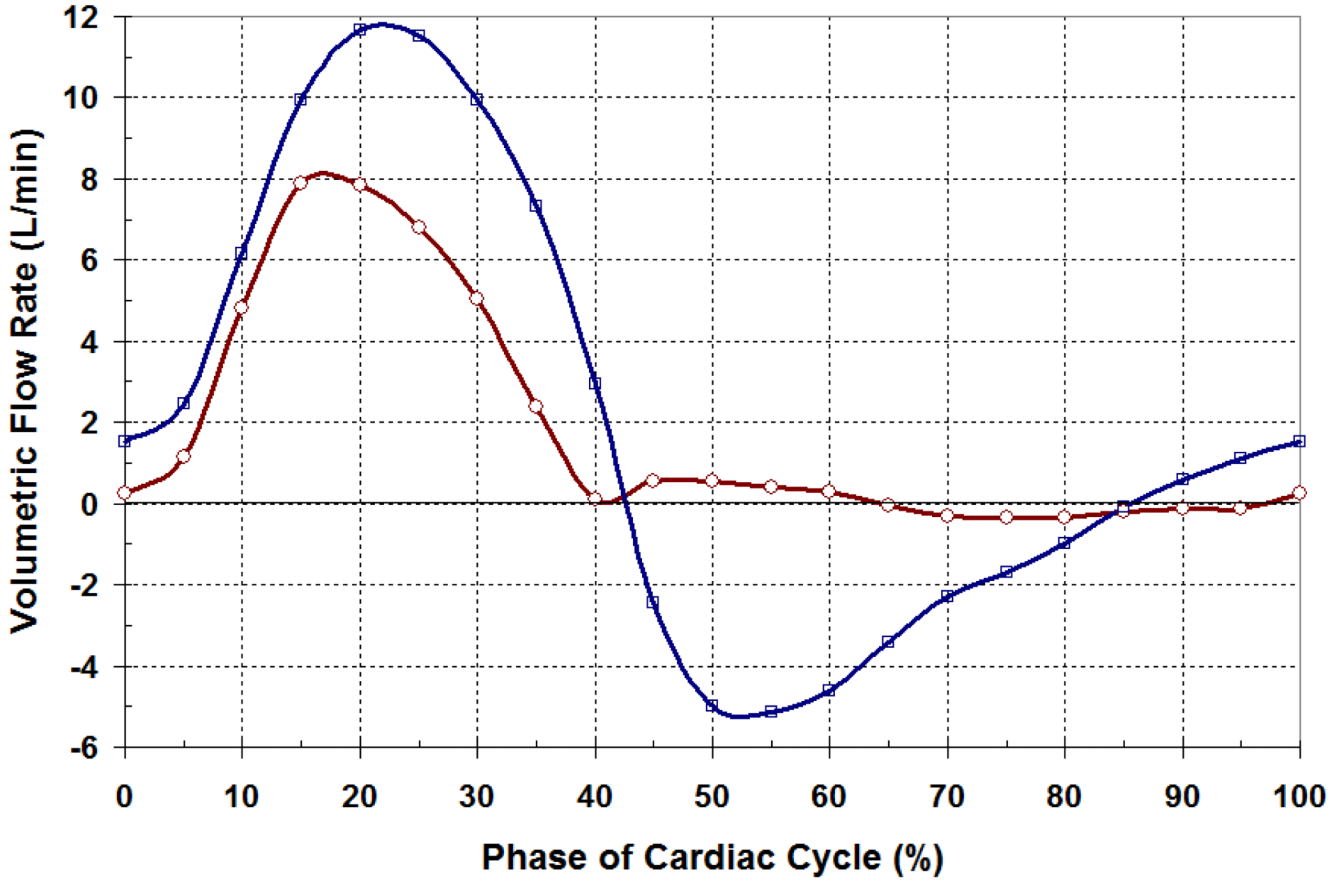

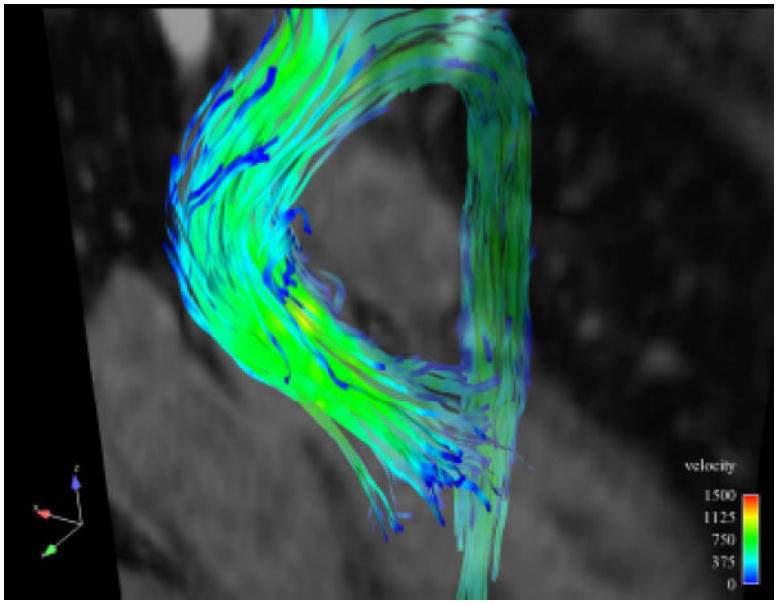

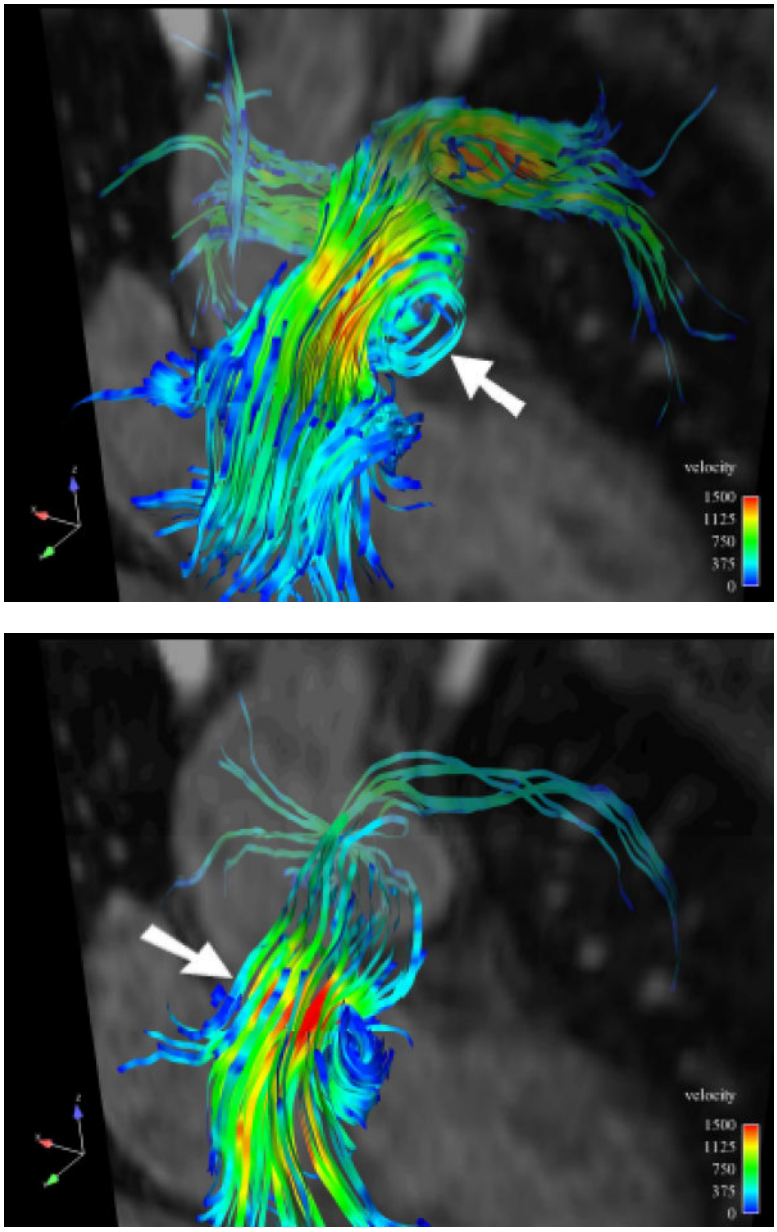

Figure 2.

Representative flow curves (a) derived from 4D flow data from a patient post-repair of tetralogy of Fallot (same patient as figure 1). The red line with open circles shows systemic flow rates (Q_s). The blue line with closed squares shows pulmonary flow rates (Q_p) with pulmonary regugitation and diastolic flow reversal marked with an arrow. Left-anterior coronal oblique views are shown of aortic streamlines at peak-systole (b), pulmonary artery streamlines in early-systole (c) and pulmonary artery streamlines in early-diastole (d). Low-speed flow is colored in blue, intermediate-speed in yellow-green, and high-speed (150 cm/s) flow in red. Streamlines are shown overlaid on a translucent coronal plane. A recirculating current is seen in the main pulmonary artery during systole, marked by an arrow. Regurgitant flow is seen during diastole, also marked by an arrow.

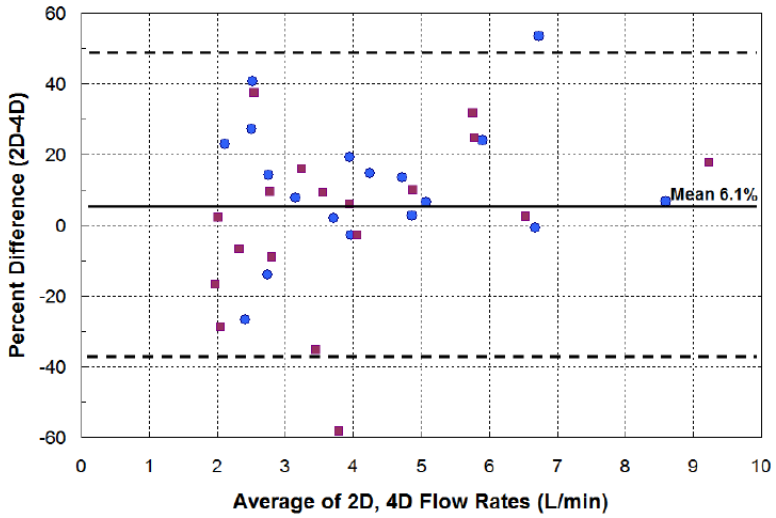

Figure 3.

Bland-Altman comparison of 2D phase-contrast and 4D phase-contrast volumetric flow rate measurements using temporally-resolved segmentations. Relative differences in flow rates are shown. Measurements of systemic flow at the aortic valve are marked by circles and measurements of pulmonary flow at the pulmonary valve are marked by squares. The outer dashed-lines indicate the limits of agreement.

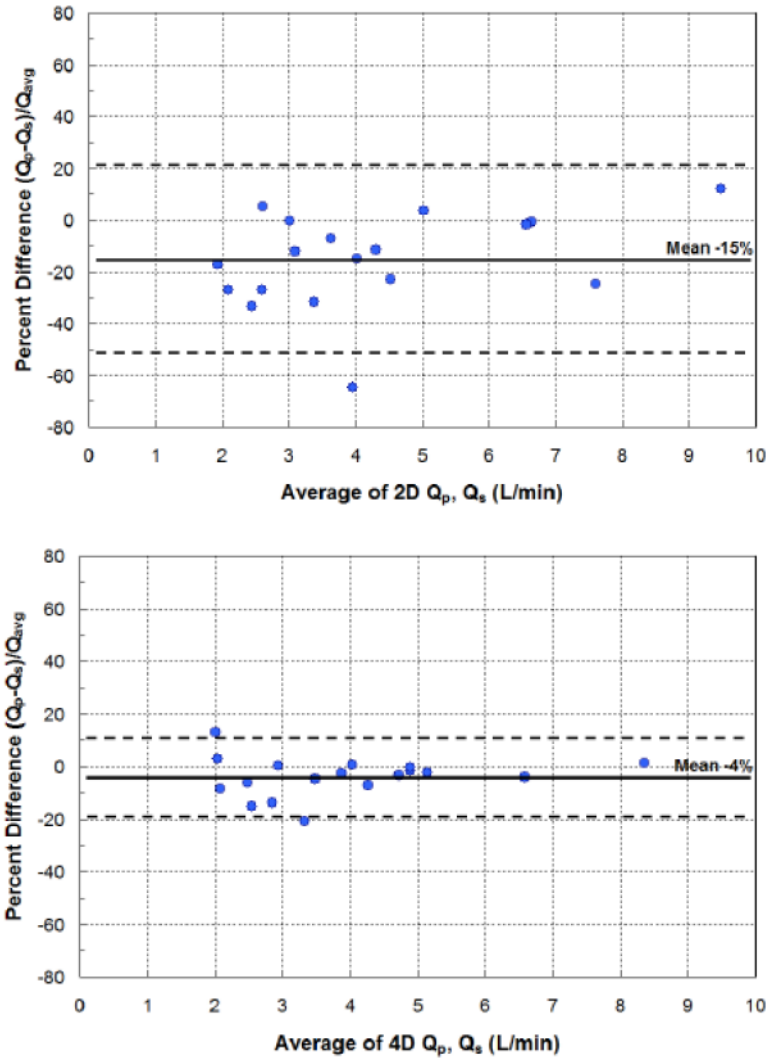

Figure 4.

Bland-Altman comparison of pulmonary (Qp) and systemic (Qs) volumetric flow rate measurements by (a) 2D phase-contrast and (b) 4D phase-contrast MRI using temporally-resolved segmentations. The outer dashed-lines indicate the limits of agreement. Note marked improvement with 4D phase-contrast, showing tighter limits and a mean difference between Q_p and Q_s closer to zero.

Pediatr Radiol. Author manuscript; available in PMC 2013 December 13.

Table 1

Patient population and acquisition parameters. The age, weight, heart rates of all patients are listed. The plane of acquisition, spatial and temporal resolution, and velocity-encoding (v_{enc}) parameters are also shown. Spatial resolution was computed based on the number of encoding steps and field of view. Temporal resolution was calculated based on TR and views per segment. The presence of valvular regurgitation with a regurgitant fraction (RF) of greater than 20% at the aortic valve (AV) or pulmonary valve (PV) is also indicated. Regurgitant fractions were measured on the 4D flow acquisition. (Abbreviations: ToF – tetralogy of Fallot, TGA – transposition of great arteries)

Pt #	Age (Y)	Wt (kg)	BSA	HR	Clinical History	RF	2D						4D					
							Resolution			v_{enc} (cm/s)		Acq. Plane	Resolution				v_{enc} (cm/s)	
							Plane (mm)	Slice (mm)	T (ms)	Ao	PA		Row (mm)	Col (mm)	Slice (mm)	T (ms)		
1	29	88	2.0	50	ToF, post-repair	PV	1.75	10	57	150	150	axial	1.84	2.19	5	42	200	
2	13	61	1.7	72	truncus arteriosis, post-repair	AV	1.38	8	36	150	300	sag	1.29	2.06	5	37	250	
3	16	99	2.2	85	hypertrophic obstructive cardiomyopathy	-	1.75	10	40	350	150	axial	1.17	2.34	5	33	400	
4	6	14	0.6	90	ToF, post-repair	PV	1.50	10	44	150	300	axial	1.02	2.03	4	37	150	
5	16	54	1.6	63	ToF, post-repair	PV	1.75	10	41	150	250	sag	1.17	2.34	4	35	250	
6	20	40	1.2	55	ToF, post-repair	-	1.25	8	33	150	350	axial	1.09	2.19	4	34	350	
7	4	14	0.6	81	ToF, post-repair	-	1.50	8	51	150	500	axial	0.94	1.88	4	34	250	
8	4	16	0.7	97	PA enlargement	-	1.50	8	45	150	150	axial	0.94	1.88	3	39	150	
9	4	20	0.8	84	d-TGA, post-Rastelli	PV	1.12	8	47	150	250	axial	1.05	2.11	3	36	300	
10	29	79	2.0	62	d-TGA, post-atrial switch	-	1.75	10	43	150	150	axial	1.17	1.88	4	35	250	
11	11	42	1.3	75	ToF, post-repair	PV	1.75	10	40	150	150	axial	1.17	1.88	4	35	250	
12	9	28	1.0	72	aortic insufficiency post-repair	AV	1.75	10	39	300	150	axial	1.17	1.88	4	34	300	
13	7	19	0.8	82	ToF, post-repair	PV	1.75	10	41	150	150	axial	1.09	1.75	3	37	200	
14	3	14	0.6	112	ToF, post-repair	PV	1.50	10	42	150	250	axial	0.86	1.38	3	37	350	
15	18	44	1.4	64	AV canal defect, post-repair	-	1.75	10	41	150	150	axial	1.17	1.88	4	35	250	
16	8	20	0.8	66	ToF, post-repair	PV	1.50	10	42	150	200	axial	0.94	1.50	3	37	250	
17	14	70	1.8	60	pulmonary stenosis, post-balloon dilation	PV	1.75	10	41	150	150	axial	1.37	2.19	4	34	250	
18	9	41	1.2	90	heart murmur, query pulmonary stenosis	-	1.38	10	47	150	150	axial	1.17	2.34	4	35	250	

Table 2

Statistical comparisons of flow measurements from 2D PC-MRI and 4D PC-MRI methods, including all systemic and pulmonary flow measurements. Flow measurements obtained by each 4D phase contrast segmentation method were on average, slightly lower than measurements by 2D PC-MRI. 4D segmentations showed tight consistency across segmentation techniques and independently-selected imaging planes. Lower limit of agreement represents the mean difference −1.96 standard deviations and upper limit of agreement represents the mean difference +1.96 standard deviations.

Method A	**4D Single Phase**	**4D Repeated**	**4D Multiple Phase**	**4D Repeated**	**4D Multiple Phase**	**4D Multiple Phase**
Method B	**2D**	**2D**	**2D**	**4D Single Phase**	**4D Single Phase**	**4D Repeated**
Pearson Correlation Coefficient	0.87	0.89	0.90	1.00	0.99	0.99
Bland-Altman Absolute Difference						
Mean difference (L/min)	0.42	0.39	0.36	−0.03	−0.06	−0.03
Lower limit of agreement (L/min)	−1.60	−1.54	−1.50	−0.33	−0.49	−0.37
Upper limit of agreement (L/min)	2.44	2.32	2.21	0.27	0.36	0.30
Bland-Altman Relative Difference						
Mean difference	8%	7%	6%	1%	−2%	−1%
Lower limit of agreement	−39%	−37%	−37%	−9%	−13%	−12%
Upper limit of agreement	55%	51%	49%	7%	9%	9%

Table 3

Statistical comparisons of pulmonary and systemic flow measurements from 2D PC-MRI and 4D PC-MRI methods in (1) all study patients and (2) patients with aortic and pulmonary valvular regurgitant fractions of less than 20%.

Including All Patients (n=18)				
	2D	**4D Single Phase**	**4D Repeated**	**4D Multiple Phase**
Pulmonary-to-systemic flow ratio: Q_p/Q_s				
Mean (standard deviation)	0.87 (0.15)	0.99 (0.11)	0.97 (0.08)	0.96 (0.07)
Bland-Altman Absolute Difference: (Q_p-Q_s, L/min)				
Mean difference (L/min)	−0.52	−0.09	−0.09	−0.14
Lower limit of agreement (L/min)	−2.10	−0.84	−0.61	−0.57
Upper limit of agreement (L/min)	1.07	0.66	0.43	0.28
Bland-Altman Relative Difference: (Q_p-Q_s)/Q_{avg}				
Mean difference	−15%	−2%	−3%	−4%
Lower limit of agreement	−51%	−23%	−18%	−19%
Upper limit of agreement	21%	19%	12%	11%
Regression: $Q_s = m \cdot Q_p + b$				
Slope (*m*)	0.86	1.04	0.99	0.98
Intercept (*b*, L/min)	1.09	−0.07	0.15	0.22
Pearson correlation (ρ)	0.93	0.98	0.99	0.99
Excluding with Less Than 20% Aortic or Pulmonary Regurgitation (n=8)				
	2D	**4D Single Phase**	**4D Repeated**	**4D Multiple Phase**
Pulmonary-to-systemic flow ratio: Q_p/Q_s				
Mean (standard deviation)	0.93 (0.13)	0.96 (0.07)	0.96 (0.06)	0.95 (0.07)
Bland-Altman Absolute Difference: (Q_p-Q_s, L/min)				
Mean difference (L/min)	−0.15	−0.20	−0.14	−0.17
Lower limit of agreement (L/min)	−1.41	−0.81	−0.56	−0.68
Upper limit of agreement (L/min)	1.11	0.40	0.27	0.34
Bland-Altman Relative Difference: (Q_p-Q_s)/Q_{avg}				
Mean difference	−8%	−5%	−5%	5%
Lower limit of agreement	−36%	−20%	−16%	−21%
Upper limit of agreement	20%	11%	7%	10%
Regression: $Q_s = m \cdot Q_p + b$				
Slope (*m*)	0.79	1.04	0.99	0.97
Intercept (*b*, L/min)	1.14	0.02	0.18	0.31
Pearson correlation (ρ)	0.99	0.99	1.00	0.99

Table 4

Statistical comparisons of Q_p-Q_s measurements from 2D and 4D PC-MRI methods with the Brown-Forsythe test, including all study patients. P-values from each test are listed. 4D PC-MRI showed statistically significant improvement in precision over 2D PC-MRI, best leveraged by either using segmentations of each cardiac phase or by taking the average of several repeated measurements along the length of the vessel.

	2D	4D Single Phase	4D Repeated
4D Single Phase	0.0868	-	-
4D Repeated	0.0206	0.1991	-
4D Multiple Phase	0.0072	0.0304	0.2321